Modelling the impact of manufacturing imperfections on photonic crystal device performance: design of perturbation-tolerant PBG components

M. Skorobogatiy[a], Steven A. Jacobs[b], Steven G. Johnson[b], M. Meunier[a], and Yoel Fink[b]

[a] École Polytechnique de Montréal, Génie physique, Montréal, QC, Canada H3C 3A7;
[b] OmniGuide Communications, One Kendall Square, Build. 100, Cambridge, MA, USA 02139

ABSTRACT

Standard perturbation theory (PT) and coupled mode theory (CMT) formulations fail or exhibit very slow convergence when applied to the analysis of geometrical variations in high index-contrast optical components such as Bragg fibers and photonic crystals waveguides. By formulating Maxwell's equations in perturbation matched curvilinear coordinates, we have derived several rigorous PT and CMT expansions that are applicable in the case of generic non-uniform dielectric profile perturbations in high index-contrast waveguides. In strong fiber tapers and fiber Bragg gratings we demonstrate that our formulation is accurate and rapidly converges to an exact result when used in a CMT framework even in the high index-contrast regime. We then apply our method to investigate the impact of hollow Bragg fiber ellipticity on its Polarization Mode Dispersion (PMD) characteristics for telecom applications. Correct PT expansions allowed us to design an efficient optimization code which we successfully applied to the design of dispersion compensating hollow Bragg fiber with optimized low PMD and very large dispersion parameter. We have also successfully extended this methodology to treat radiation scattering due to common geometric variations in generic photonic crystals. As an example, scattering analysis in strong 2D photonic crystal tapers is demonstrated.

Keywords: photonic crystals, microstructured fibers, perturbation theory, coupled mode theory, imperfections

1. INTRODUCTION

Standard perturbation and coupled mode theory formulations are known to fail or exhibit a very slow convergence[1–6] when applied to the analysis of geometrical variations in the structure of high index-contrast fibers. In a uniform coupled mode theory framework (waveguide profile remains unchanged along the direction of propagation), eigenvalues of the matrix of coupling elements approximate the values of the propagation constants of a uniform waveguide of perturbed cross-section. When large enough number of modes are included coupled mode theory, in principle, should converge to an exact solution for perturbations of any strength. Perturbation theory is numerically more efficient method than coupled mode theory, but it is mostly applicable to the analysis of small perturbations. For stronger perturbations, higher order perturbation corrections must be included converging, in the limit of higher orders, to an exact solution. In a non-uniform (waveguide profile is changing along the direction of propagation) coupled mode and perturbation theories one propagates the modal coefficients along the length of a waveguide using a first order differential equation involving a matrix of coupling elements. Both uniform and non-uniform coupled mode and perturbation theory expansions rely on the knowledge of correct coupling elements.

Conventional approach to the evaluation of the coupling elements proceeds by expansion of the solution for the fields in a perturbed waveguide into the modes of an unperturbed system, then computes a correction to the Hamiltonian of a problem due to the perturbation in question and, finally, computes the required coupling elements. Unfortunately, this approach encounters difficulties when applied to the problem of finding perturbed electromagnetic modes in the waveguides with shifted high index-contrast dielectric boundaries. In particular,

---

Send e-mail to: maksim.skorobogatiy@polymtl.ca

it was demonstrated[3] that for a uniform geometric perturbation of a fiber profile with abrupt high index-contrast dielectric interfaces, expansion of the perturbed modes into an increasing number of the modes of an unperturbed system does not converge to a correct solution when standard form of the coupling elements[7,8] is used. Mathematical reasons of such a failure are still not completely understood but probably lie either in the *incompleteness* of the basis of eigenmodes of an unperturbed waveguide in the domain of the eigenmodes of a perturbed waveguide or in the fact that the standard mode orthogonality conditions (4.1) do not constitute strict norms. We would like to point out that standard coupled mode theory can still be used even in the problem of finding the modes of a high index-contrast waveguide with sharp dielectric interfaces. One can calculate such modes by using as an expansion basis eigen modes of some "smooth" dielectric profile (empty metallic waveguide, for example). However, the convergence of such a method with respect to the number of basis modes is slow (linear). Perturbation formulation within this approach is also problematic, and even for small geometric variations of waveguide profile matrix of coupling element has to be recomputed anew. Other methods developed to deal with shifting metallic boundaries and dielectric interfaces originate primarily from the works on metallic waveguides and microwave circuits.[7,9–13] Dealing with non-uniform waveguides, these formulations usually employ an expansion basis of "instantaneous modes". Such modes have to be recalculated at each different waveguide cross-section leading to potentially computationally demanding propagation schemes.

In this paper we introduce a method of evaluating the coupling elements which is valid for any analytical geometrical waveguide profile variations and high index contrast using the eigen modes of an waveguide unperturbed (to which we refer as a basic waveguide) as an expansion basis. Main idea of our method is to introduce a coordinate transformation that maps a dielectric profile of a perturbed waveguide onto a dielectric profile of a basic waveguide whose eigen modes are assumed to be known. Transforming Maxwell's equations into a curvilinear system where dielectric profile is unperturbed we can use the eigen modes of a basic waveguide as an expansion basis. These modes will be now coupled due to the curvature of the space which is in turn proportional to the strength of the perturbation in question. In further discussions we formulate geometrical waveguide profile variations in terms of an analytical mapping of a unperturbed dielectric profile onto a perturbed one. Given a perturbed dielectric profile $\epsilon(x, y, z)$ in a Euclidian system of coordinates (x, y, z) (where z is a general direction of propagation) we define a mapping $(x(q^1, q^2, s), y(q^1, q^2, s), z(q^1, q^2, s))$ such that $\epsilon(q^1, q^2, s)$ corresponds to a dielectric profile of a basic waveguide in a curvilinear coordinate system associated with (q^1, q^2, s) (where s is a strict direction of propagation). We then perform a coordinate transformation from a Euclidian system of coordinates (x, y, z) into a corresponding curvilinear coordinate system (q^1, q^2, s) by rewriting Maxwell's equations in such a coordinate system. Finally, as the dielectric profile in a coordinate system (q^1, q^2, s) is that of an basic waveguide, we can use the basis set of its eigen modes in (q^1, q^2, s) coordinates to calculate coupling matrix elements due to the geometrical perturbation of a waveguide profile.

Our paper is organized as following. We first describe some typical geometrical variations of waveguide profiles. Next, we discuss properties of generic curvilinear coordinate transformations and formulate Maxwell's equations in a curvilinear coordinate system. We apply this formulation to develop the coupled mode and perturbation theories using eigen states of an unperturbed waveguide as an expansion basis. We conclude with a variety of application in photonic crystal fibers and 2D waveguides.

2. GEOMETRICAL VARIATIONS OF WAVEGUIDE PROFILES

We start by considering some common geometrical variations of waveguide profiles that can be either deliberately designed or arise during manufacturing as perturbations. Let (x, y, z) correspond to Euclidian coordinate system. In cylindrical coordinates $x = \rho Cos(\theta), y = \rho Sin(\theta), z = s$. Then, for the step-index multilayer fibers, for example, the position of the $i'th$ dielectric interface of radius ρ_i can be described by a set of points, $\rho = \rho_i, \theta \in (0, 2\pi)$ (see Fig. 1a)). Geometrical variations in multilayer fibers that will be considered in this paper for the purpose of demonstration of our method include high index contrast Bragg gratings, tapers and uniform ellipticity. If all the radii of the dielectric interfaces are scaled from their original values ρ_i to become $\rho_i(1 + f(s))$ where $f(s)$ is an analytic function of propagation distance s, then the following coordinate mapping will describe such a scaling variation of interface radii along the direction of propagation $x = \rho Cos(\theta)(1 + f(s)), y = \rho Sin(\theta)(1 + f(s)), z = s$. Here, $\rho = \rho_i, \theta \in (0, 2\pi)$ define the points on the $i'th$ unperturbed dielectric interface, while the corresponding $(x(\rho, \theta, s), y(\rho, \theta, s), z(\rho, \theta, s))$ describe the points on the perturbed
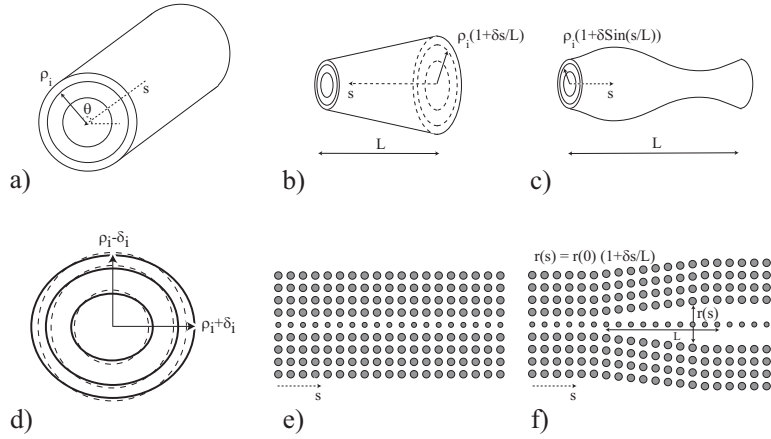
Figure 1. a) Dielectric profile of an ideal cylindrically symmetric fiber. Concentric dielectric interfaces are characterized by their radii ρ_i. b) Scaling variation - linear taper. Fiber profile remains cylindrically symmetric, while the radii of the dielectric interfaces along the direction of propagation s become $\rho_i(1 + \delta\frac{s}{L})$. c) Scaling variation - sinusoidal Bragg grating. Fiber profile remains cylindrically symmetric, while the radii of the dielectric interfaces along the direction of propagation s become $\rho_i(1 + \delta Sin(2\pi\frac{s}{\Lambda}))$. d) Uniform fiber ellipticity. e) Dielectric profile of an ideal 2D photonic crystal waveguide as formed by a linear sequence of somewhat smaller dielectric poles in a square array of larger dielectric poles in the air. f) Linear taper in the photonic crystal with "unzipping" photonic mirror.[13]

interfaces. Using thus introduced coordinate transformation we can introduce several common optical elements. One of them is a taper described by the monotonic variations in the radii of the dielectric layers in a cylindrically symmetric fiber (Fig. 1b)). In the case of a linear taper $f(s) = \delta\frac{s}{L}$ where L is a length of a taper and δ is a relative change in the taper dimensions from the beginning to the end. Another element is a dielectric Bragg grating of any strength, where the radii of the dielectric layers change according to some analytic periodic function along the direction of propagation in a cylindrically symmetric fiber (Fig. 1c)). In the case of a sinusoidal grating, for example, $f(s) = \delta sin(2\pi\frac{s}{\Lambda})$, where δ defines the magnitude of the radial variation of the grating dimensions, while Λ corresponds to the pitch of the grating. In the same manner as for the case of concentric perturbations, we can define non-concentric perturbations through the respective coordinate transformation. Thus, uniform fiber ellipticity (Fig. 1d)) of the dielectric interfaces can be defined as $x = \rho Cos(\theta)(1 + \delta f(\rho)), y = \rho Sin(\theta)(1 - \delta f(\rho)), z = s$. In the same manner, variations in planar geometries can be defined through the corresponding coordinate mapping. On Fig. 1e) an ideal 2D photonic crystal waveguide is presented, while on Fig. 1f) the photonic crystal taper with "unzipping" mirror is presented. In the last section of this paper we will show how to define a corresponding mapping from e) to f). In more complicated geometries, coordinate mappings can be computed numerically from the original and final position of the dielectric interfaces.

3. CURVILINEAR COORDINATE SYSTEMS

Following,[14, 15] we first introduce general properties of the curvilinear coordinate transformations. Let (x^1, x^2, x^3) be the coordinates in a Euclidian coordinate system. We introduce an analytical mapping into a new coordinate system with coordinates (q^1, q^2, q^3) as $(x^1(q^1, q^2, q^3), x^2(q^1, q^2, q^3), x^3(q^1, q^2, q^3))$. A new coordinate system can be characterized by its covariant basis vectors $\vec{a}_i$ defined in the original Euclidian system as $\vec{a}_i = (\frac{\partial x^1}{\partial q^i}, \frac{\partial x^2}{\partial q^i}, \frac{\partial x^3}{\partial q^i})$. Now, define reciprocal (contravariant) vector $\vec{a}^i$ as $\quad \vec{a}^i = \frac{1}{\sqrt{g}}\vec{a}_j \times \vec{a}_k, \quad (k, j) \neq i$, where metric g_{ij} is defined as $g_{ij} = \frac{\partial x^k}{\partial q^i}\frac{\partial x^k}{\partial q^j}$, and $g = det(g_{ij})$. Vectors $\vec{a}_i$ and their reciprocal $\vec{a}^i$ satisfy the following orthogonality conditions $\vec{a}^i \cdot \vec{a}_j = \delta_{i,j} \quad , \quad \vec{a}_i \cdot \vec{a}_j = g_{ij} \quad , \quad \vec{a}^i \cdot \vec{a}^j = g^{ij}$, where g^{ij} is an inverse of the metric g_{ij}. In general, a vector may be represented by its covariant components $\vec{E} = e_i\vec{a}^i$ or by its contravariant components $\vec{E} = e^i\vec{a}_i$. These components might have unusual dimensions because the underlying vectors $\vec{a}_i$ and $\vec{a}^i$ are not properly normalized in a Euclidian coordinate system. Components having the usual dimensions are defined by $E_i = \frac{e_i}{\sqrt{g^{ii}}}$, $E^i = \frac{e^i}{\sqrt{g_{ii}}}$ and $\vec{E} = e_i\vec{a}^i = E_i\vec{i}^i, \vec{E} = e^i\vec{a}_i = E^i\vec{i}_i$, where $\vec{i}_i, \vec{i}^i$ are unitary vectors. Normalized covariant and

contravariant components are connected by $E_i = G_{ij}E^j$, $E^i = G^{ij}E_j$ where $G_{ij} = \sqrt{\frac{g^{ii}}{g_{jj}}}g_{ij}$, $G^{ij} = \sqrt{\frac{g_{ii}}{g^{jj}}}g^{ij}$. For orthogonal coordinate systems the metric matrixes are diagonal and for the regular orthogonal and polar coordinate systems they are $g^{0xx} = 1; g^{0yy} = 1; g^{0zz} = 1; g^0 = 1$, and $g^{0\rho\rho} = 1; g^{0\theta\theta} = \frac{1}{\rho^2}; g^{0zz} = 1; g^0 = \rho^2$ correspondingly.

4. COUPLED MODE THEORY FOR MAXWELL'S EQUATIONS IN CURVILINEAR COORDINATES

In the following, we summarize coupled mode theory for Maxwell's equations in curvilinear coordinates to treat radiation propagation in generic non-uniform waveguides. Hamiltonian formulation of Maxwell's equations in regular Euclidian coordinates is detailed in,[3, 13] while Hamiltonian formulation and coupled mode theory in curvilinear perturbation matched coordinates for the case of uniform and non-uniform fibers of arbitrary cross-sections is detailed in.[3, 4, 18]

The form of Maxwell's equations in curvilinear coordinates can be found in a variety of references.[14–17] Assuming the standard time dependence of the electro-magnetic fields $\mathbf{F}(q_1, q_2, q_3, t) = \mathbf{F}(q_1, q_2, q_3) \exp(-i\omega t)$, ($\mathbf{F} = (\frac{E_{q_1}}{\sqrt{g^{11}}}; \frac{E_{q_2}}{\sqrt{g^{22}}}; \frac{E_{q_3}}{\sqrt{g^{33}}}; \frac{H_{q_1}}{\sqrt{g^{11}}}; \frac{H_{q_2}}{\sqrt{g^{22}}}; \frac{H_{q_3}}{\sqrt{g^{33}}})$ denotes a 6 component column vector of the electro-magnetic fields) these expressions are compactly presented in terms of the normalized covariant components of the fields, and in the absence of free electric currents they are:

$$
\begin{aligned}
-i\omega\epsilon(q^1, q^2, q^3)D^{ij}\frac{E_j}{\sqrt{g^{jj}}} &= e^{ijk}\frac{\partial \frac{H_k}{\sqrt{g^{kk}}}}{\partial q^j} \\
i\omega\mu(q^1, q^2, q^3)D^{ij}\frac{H_j}{\sqrt{g^{jj}}} &= e^{ijk}\frac{\partial \frac{E_k}{\sqrt{g^{kk}}}}{\partial q^j},
\end{aligned}
\tag{1}
$$

where $D^{ij} = \sqrt{g}g^{ij}$, and e^{ijk} is a Levi-Civita symbol.

4.1. Modal orthogonality relations and normalization

In the following we assume that unperturbed waveguide is either uniform (planar waveguide, fiber) or strictly periodic (photonic crystal waveguide, fiber grating) along the direction of propagation $q^3 = s$. This implies that both ϵ_0 and μ_0 (marking parameters related to basic waveguide with a subscript zero) either do not depend on s, or they are periodic functions of s. We assume that eigen modes and eigen values of a basic waveguide are found in a coordinate system with a diagonal space metric (orthogonal coordinate system). Several orthogonality relations between the eigen modes of a basic waveguide are possible.

If unperturbed waveguide profile is uniform along s, then the eigen fields have an additional symmetry $\mathbf{F}(q^1, q^2, s) = \mathbf{F}_\beta(q^1, q^2) \exp(i\beta s)$. Introducing a norm operator $\hat{B}$ as a 6X6 matrix with 4 non-zero elements[13] $B(1,5) = B(5,1) = -B(2,4) = -B(4,2) = 1$, which relates transverse components of the fields, we derive:
1) If ϵ_0 and μ_0 are strictly real we introduce Dirac notation as $|\beta\rangle = \mathbf{F}_\beta(q^1, q^2)$ and $\langle\beta| = \mathbf{F}_\beta^*(q^1, q^2)$, and a product operator $\langle\beta_i|\hat{O}|\beta_j\rangle = \int_{cros} dq^1 dq^2 \mathbf{F}_{\beta_i}^+(q^1, q^2)O\mathbf{F}_{\beta_j}(q^1, q^2)$, where O is a 6X6 operator matrix, and integration is performed over the waveguide crossection. Then for any two eigen modes labelled by their propagation constants β_i, β_j the eigen modes can be normalized as $\langle\beta_i|B|\beta_j\rangle = \delta_{\beta_i^*, \beta_j}\eta_{\beta_j}$, and $|\eta_{\beta_j}| = 1$.
2) If ϵ_0 and μ_0 are not strictly real, we introduce Dirac notation as $|\beta\rangle = \mathbf{F}_\beta(q^1, q^2)$ and $\langle\beta| = \mathbf{F}_\beta(q^1, q^2)$, (no complex conjugation) and a product operator $\langle\beta_i|\hat{O}|\beta_j\rangle = \int_{cros} dq^1 dq^2 \mathbf{F}_{\beta_i}^T(q^1, q^2)O\mathbf{F}_{\beta_j}(q^1, q^2)$, where integration is performed over the waveguide crossection. Then for any two eigen modes labelled by their propagation constants β_i, β_j the eigen modes can be normalized as $\langle\beta_i|B|\beta_j\rangle = \delta_{\beta_i, \beta_j}\eta_{\beta_j}$, and $|\eta_{\beta_j}| = 1$.

If unperturbed waveguide profile is periodic along s with period Λ then according to the Bloch-Floquet theorem the eigen fields still retain a symmetry $\mathbf{F}(q^1, q^2, s) = \mathbf{F}_\beta(q^1, q^2, s) \exp(i\beta s)$, where $\mathbf{F}_\beta(q^1, q^2, s) = \mathbf{F}_\beta(q^1, q^2, s + \Lambda)$. If ϵ_0 and μ_0 are strictly real we introduce Dirac notation as $|\beta\rangle = \mathbf{F}_\beta(q^1, q^2, s)$ and $\langle\beta| = \mathbf{F}_\beta^*(q^1, q^2, s)$, as well as a product operator $\langle\beta_i|\hat{O}|\beta_j\rangle = \int_{cell} dq^1 dq^2 ds \mathbf{F}_{\beta_i}^+(q^1, q^2, s)O\mathbf{F}_{\beta_j}(q^1, q^2, s)$, where O is a 6X6 operator matrix and integration is performed over the whole unit cell of a periodic waveguide. Then for any two eigen modes labelled by their propagation constants β_i, β_j the eigen modes can be normalized as

$\langle\beta_i|B|\beta_j\rangle = \delta_{\beta_1^*,\beta_j}\eta_{\beta_j}$, and $|\eta_{\beta_j}| = 1$. Moreover, a corollary of Bloch-Floquet theorem states that the eigen modes at β and $\beta + 2\pi l/\Lambda$ are equivalent for any integer l, and thus $|\beta + 2\pi l/\Lambda\rangle = \exp(-2\pi i l/\Lambda z)|\beta\rangle$. This implies that it suffices to choose all the eigen values β in the first Brillouin zone $Re(\beta) \in (-\pi/\Lambda, \pi/\Lambda]$, and for such modes definition of the norm can be furthermore relaxed to be $\langle\beta_i|\hat{O}|\beta_j\rangle = \int_{cell} dq^1 dq^2 ds \mathbf{F}_{\beta_i}^+(q^1, q^2, s)O\mathbf{F}_{\beta_j}(q^1, q^2, s) = \Lambda \int_{cros} dq^1 dq^2 \mathbf{F}_{\beta_i}^+(q^1, q^2, s)O\mathbf{F}_{\beta_j}(q^1, q^2, s)$, where the integral over waveguide crossection is invariant for any crossection (any s) in the first Brilloun zone. Thus, definition of the norm in the case of real ϵ_0 and μ_0 for periodic or uniform waveguides can be chosen to be the same.

4.2. Expansion basis

We now construct an expansion basis to treat radiation propagation in a perturbed waveguide using the eigen fields of an unperturbed waveguide in the perturbation matched curvilinear coordinate system. Equivalently, in the Euclidian coordinate system associated with a perturbed waveguide we construct an expansion basis from the eigen fields of an unperturbed waveguide by spatially stretching them in such a way as to match the regions of discontinuity of their field components with the position of the perturbed dielectric interfaces. Finally, we find expansion coefficients by satisfying Maxwell's equations. In the following, we first define an expansion basis and then demonstrate how perturbation theory and a coupled mode theory can be formulated in such a basis.

Let (x, y, z) to define a Euclidian coordinate system associated with a perturbed waveguide, and (q^1, q^2, s) be a coordinate system corresponding to an unperturbed waveguide, where s is a direction of propagation, with corresponding coordinate transformation relating the two coordinate systems being $(x(q^1, q^2, s), y(q^1, q^2, s), z(q^1, q^2, s))$. Using transverse eigen fields of a basic waveguide expressed in the coordinates (q^1, q^2, s) we form an expansion basis in the Euclidian coordinate system (x, y, z) as following:

$$|\Psi_\beta\rangle = \left(\begin{array}{c} \frac{E_{q^1}^0(q^1(x,y,z),q^2(x,y,z),s(x,y,z))}{\sqrt{g^{0q^1q^1}}}\vec{i}^{q^1} + \frac{E_{q^2}^0(q^1(x,y,z),q^2(x,y,z),s(x,y,z))}{\sqrt{g^{0q^2q^2}}}\vec{i}^{q^2} \\ \frac{H_{q^1}^0((q^1(x,y,z),q^2(x,y,z),s(x,y,z))}{\sqrt{g^{0q^1q^1}}}\vec{i}^{q^1} + \frac{H_{q^2}^0(q^1(x,y,z),q^2(x,y,z),s(x,y,z))}{\sqrt{g^{0q^2q^2}}}\vec{i}^{q^2} \end{array} \right)_\beta. \tag{2}$$

There are several important properties that basis vector fields (2) possess. First, if coordinate transformation is orthogonal ($\vec{i}^{q\{1,2,3\}} = \vec{i}_{q\{1,2,3\}}$) then one can show that any two basis fields of (2) are orthogonal in a sense of the orthogonality condition discussed in (4.1). Moreover, in the case of non-orthogonal transformations, basis fields (2) will be almost orthogonal with an amount of non-orthogonality proportional to the strength of perturbation. Second, regions of discontinuity in the field components of the basis fields (2), by construction, coincide with the positions of the perturbed dielectric interfaces.

4.3. Coupled mode theory

Maxwell's equations in curvilinear coordinates (1), while seemingly complicated, involve an unperturbed dielectric profile $\epsilon(q^1, q^2, s)$. We look for a solution of Maxwell's equations (1) in terms of the basis fields (2) which in (q^1, q^2, s) coordinate system are the eigen fields of a basic waveguide entering with corresponding varying along the direction of propagation coefficients $C^\beta(s)$. Thus, in the covariant coordinates for both uniform and periodic waveguides we look for a solution in a form:

$$\left(\begin{array}{c} \frac{E_{q^1}(q^1,q^2,s)}{\sqrt{g^{q^1q^1}}} \\ \frac{E_{q^2}(q^1,q^2,s)}{\sqrt{g^{q^2q^2}}} \\ \frac{H_{q^1}(q^1,q^2,s)}{\sqrt{g^{q^1q^1}}} \\ \frac{H_{q^2}(q^1,q^2,s)}{\sqrt{g^{q^2q^2}}} \end{array} \right) = \sum_{\beta_j} C^{\beta_j}(s) \left(\begin{array}{c} \frac{E_{q^1}^0(q^1,q^2,s)}{\sqrt{g^{0q^1q^1}}} \\ \frac{E_{q^2}^0(q^1,q^2,s)}{\sqrt{g^{0q^2q^2}}} \\ \frac{H_{q^1}^0(q^1,q^2,s)}{\sqrt{g^{0q^1q^1}}} \\ \frac{H_{q^2}^0(q^1,q^2,s)}{\sqrt{g^{0q^2q^2}}} \end{array} \right)_{\beta_j}. \tag{3}$$

Note, that for a uniform basic waveguide, the expansion fields (2) are functions of (q^1, q^2) only, and in both cases of periodic and uniform waveguides basis fields are stripped of the phase factor $\exp(i\beta z)$. Substituting

expansion (3) into (1), expressing s components of the fields through the transverse components, using the orthogonality relations (4.1) and manipulating the resultant expressions we arrive to the following equations:

$$B\frac{\partial\vec{C}(s)}{\partial s} = i(\mathcal{B}_0 + \Delta M(s))\vec{C}(s), \tag{4}$$

where $B_{\beta_i,\beta_j} = \langle\beta_i|\hat{B}|\beta_j\rangle$ is a constant normalization matrix, $\mathcal{B}_0$ is a diagonal matrix of eigenvalues of an unperturbed waveguide, and $\Delta M(s)$ is a matrix of coupling elements given by

$$\Delta M_{\beta_i,\beta_j}(s) =$$

$$\frac{\omega}{c}\int dq^1 dq^2 \begin{pmatrix} \frac{E^0_{q^1}(q^1,q^2,s)}{\sqrt{g^{0q^1q^1}}} \\ \frac{E^0_{q^2}(q^2,q^2,s)}{\sqrt{g^{0q^2q^2}}} \\ \frac{E^0_s(q^1,q^2,s)}{\sqrt{g^{0ss}}} \\ \frac{H^0_{q^1}(q^1,q^2,s)}{\sqrt{g^{0q^1q^1}}} \\ \frac{H^0_{q^2}(q^1,q^2,s)}{\sqrt{g^{0q^2q^2}}} \\ \frac{H^0_s(q^1,q^2,s)}{\sqrt{g^{0ss}}} \end{pmatrix}_{\beta_i}^{\dagger,T} \begin{pmatrix} d\epsilon_{q^1q^1} & d\epsilon_{q^1q^2} & d\epsilon_{q^1s} & 0 & 0 & 0 \\ d\epsilon_{q^2q^1} & d\epsilon_{q^2q^2} & d\epsilon_{q^2s} & 0 & 0 & 0 \\ d\epsilon_{sq^1} & d\epsilon_{sq^2} & d\epsilon_{ss} & 0 & 0 & 0 \\ 0 & 0 & 0 & d\mu_{q^1q^1} & d\mu_{q^1q^2} & d\mu_{q^1s} \\ 0 & 0 & 0 & d\mu_{q^2q^1} & d\mu_{q^2q^2} & d\mu_{q^2s} \\ 0 & 0 & 0 & d\mu_{sq^1} & d\mu_{sq^2} & d\mu_{ss} \end{pmatrix} \begin{pmatrix} \frac{E^0_{q^1}(q^1,q^2,s)}{\sqrt{g^{0q^1q^1}}} \\ \frac{E^0_{q^2}(q^2,q^2,s)}{\sqrt{g^{0q^2q^2}}} \\ \frac{E^0_s(q^1,q^2,s)}{\sqrt{g^{0ss}}} \\ \frac{H^0_{q^1}(q^1,q^2,s)}{\sqrt{g^{0q^1q^1}}} \\ \frac{H^0_{q^2}(q^1,q^2,s)}{\sqrt{g^{0q^2q^2}}} \\ \frac{H^0_s(q^1,q^2,s)}{\sqrt{g^{0ss}}} \end{pmatrix}_{\beta_j}, \tag{5}$$

where integration is performed over an unperturbed waveguide profile, complex conjugation should be chosen for real ϵ_0 and μ_0 uniform or periodic unperturbed waveguides, while unconjugated product can be used with uniform waveguides and complex ϵ_0 and μ_0 as described in (4.1). Assuming that eigen fields of unperturbed waveguide were found in a diagonal metric, non-zero elements of 6×6 matrix $\Delta\hat{M}(s)$ are

$$\begin{aligned}
d\epsilon_{q^1q^1} &= \epsilon D^{q^1q^1} - \epsilon_0 D_0^{q^1q^1} - \epsilon\frac{(D^{q^1s})^2}{D_{ss}} & d\mu_{q^1q^1} &= \mu D^{q^1q^1} - \mu_0 D_0^{q^1q^1} - \mu\frac{(D^{q^1s})^2}{D_{ss}} \\
d\epsilon_{q^1q^2} &= d\epsilon_{q^2q^1} = \epsilon(D^{q^1q^2} - \frac{D^{q^1s}D^{q^2s}}{D_{ss}}) & d\mu_{q^1q^2} &= d\mu_{q^2q^1} = \mu(D^{q^1q^2} - \frac{D^{q^1s}D^{q^2s}}{D_{ss}}) \\
d\epsilon_{q^1s} &= d\epsilon_{sq^1} = \epsilon_0\frac{D^{q^1s}D_0^{ss}}{D_{ss}} & d\mu_{q^1s} &= d\mu_{sq^1} = \mu_0\frac{D^{q^1s}D_0^{ss}}{D_{ss}} \\
d\epsilon_{q^2q^2} &= \epsilon D^{q^2q^2} - \epsilon_0 D_0^{q^2q^2} - \epsilon\frac{(D^{q^2s})^2}{D_{ss}} & d\mu_{q^2q^2} &= \mu D^{q^2q^2} - \mu_0 D_0^{q^2q^2} - \mu\frac{(D^{q^2s})^2}{D_{ss}} \\
d\epsilon_{q^2s} &= d\epsilon_{sq^2} = \epsilon_0\frac{D^{q^2s}D_0^{ss}}{D_{ss}} & d\mu_{q^2s} &= d\mu_{sq^2} = \mu_0\frac{D^{q^2s}D_0^{ss}}{D_{ss}} \\
d\epsilon_{ss} &= \epsilon_0 D_0^{ss}(1 - \frac{\epsilon_0 D_0^{ss}}{\epsilon D^{ss}}) & d\mu_{ss} &= \mu_0 D_0^{ss}(1 - \frac{\mu_0 D_0^{ss}}{\mu D^{ss}}).
\end{aligned} \tag{6}$$

where ϵ and μ describe the profile of a perturbed waveguide (case $\epsilon = \epsilon_0$ and $\mu = \mu_0$ corresponds to the shifting material boundaries), and $D_{ij} = \sqrt{g}g^{ij}$. Note that the matrix of coupling elements $\Delta M(s)$ is symmetric/Hermitian depending upon the choice of normalization. Equations (4) present a system of first order linear coupled differential equations with respect to a vector of expansion coefficients $C^\beta(s)$. Boundary conditions such as modal content of an incoming and an outgoing signal define a boundary value problem that can be further solved numerically.

Presented coupled mode theory describes completely radiation scattering in arbitrary index-contrast waveguides with shifting dielectric boundaries and changing dielectric profile. Moreover, (4) allows perturbative expansions. As a metric of a slightly perturbed coordinate system in only slightly different from the metric of an unperturbed coordinate system that will naturally introduce a small parameter for small geometrical perturbations of waveguide profiles.

5. CONVERGENCE OF THE COUPLED MODE THEORY

We test our theory on a set of geometrical variations in the all-dielectric high index-contrast waveguides. First we consider long and short tapers and a limiting case of an abrupt junction between two fibers. Next, we consider strong fiber Bragg gratings. An underlying basic waveguide used in our study is a single core high
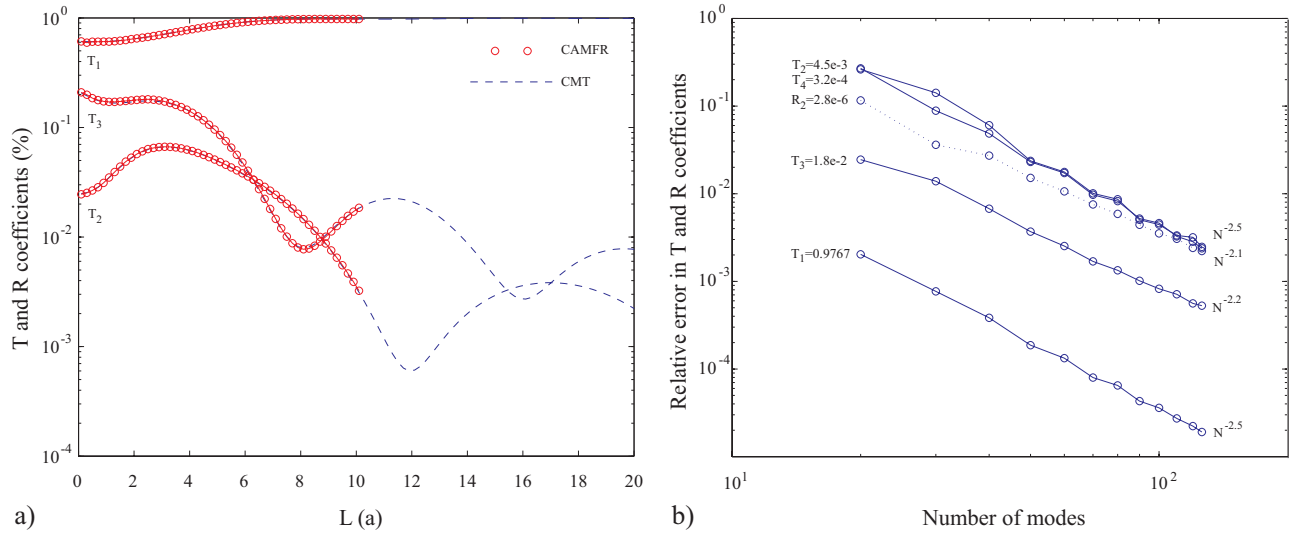
Figure 2. a) Transmitted power T_1 in the fundamental $m = 1$ mode, and in the second and third $m = 1$ parasitic modes T_2, T_3 as a function of the taper length L, calculated by the developed CMT. Results of an asymptotically exact transfer matrix based CAMFR code are presented in circles. b) Convergence of the relative errors in the transmitted and reflected coefficients for a taper length of $L = 10a$ as a function of the number of expansion modes. Solid lines correspond to the relative errors in the transmission coefficients while dotted lines correspond to the relative errors in the reflected coefficients. Errors in the transmission and reflection coefficients exhibit faster than a quadratic convergence.

index-contrast waveguide of radius $R_{core} = 1.525a$, $n_{core} = 3$, $n_{clad} = 1$ surrounded by a metallic jacket of $R_{metal} = 4a$. Frequency of operation is fixed and equal $\omega = 0.2\frac{2\pi c}{a}$, propagation constant is measured in units $\frac{2\pi}{a}$, where a defines the scale and can be chosen at will. There are altogether 10 - $m = 0$, 16 - $m = \pm 1$, 12 - $m = \pm 2$ and 8 - $m = \pm 3$ guided modes in this fiber. Metallic boundary conditions due to a waveguide outer jacket eliminate the radiation continuum leaving a discrete spectrum of guided (propagation constant is pure real) and evanescent modes (propagation constant is pure imaginary).

First, we consider a linear taper variation of a waveguide profile where all the interfaces (including an outside metal jacket) are scaled by the same amount along the direction of propagation (see Fig. 1b)). A corresponding coordinate mapping will be that of (2) with $f(s) = \delta\frac{s}{L}$, where L is a length of a taper, and δ is its strength. For a strong taper variation of $\delta = 1$ and a boundary condition of all the incoming radiation coming in the fundamental $m = 1$ mode we solve (4) for the power in the transmitted and reflected modes propagating in the incoming and outgoing waveguides. We assume propagation from a larger waveguide into a smaller basic waveguide. Expansion basis consisted of 8 - $m = 1$ guided and 42 - $m = 1$ evanescent modes of an outgoing basic waveguide. On Fig. 2a) we plot in dotted lines a transmitted power T_1 in the fundamental $m = 1$ mode, along with the transmitted powers T_2, T_3 in the second and third $m = 1$ parasitic modes as a function of the taper length L, and calculated by our coupled mode theory . For comparison, results of an asymptotically exact transfer matrix based CAMFR code[19] are presented on the same figure in circles exhibiting an excellent agreement with our results. When taper length goes to zero we retrieve the case of an abrupt junction between different waveguides. In the case when taper length is large enough we are in the regime of a standard taper with most of the transmitted power staying in the same mode. On Fig. 2b), we present convergence of the transmitted and reflected coefficients for a linear taper of length $L = 10a$. Solid lines correspond to the relative errors in the transmission coefficients while dotted lines correspond to the relative errors in the reflected coefficients. Note a very robust convergence of our coupled mode theory with respect to the number of modes in the expansion basis. Errors in the coefficients exhibit faster than quadratic convergence. For comparison, standard coupled mode theory dealing with perturbed high index contrast discontinuous interfaces either does not converges at all or exhibit a very slow linear convergence of errors.[2,4] We also observe that in all the regimes of short and long taper lengths our coupled mode theory gives the correct values of the main transmission and reflection
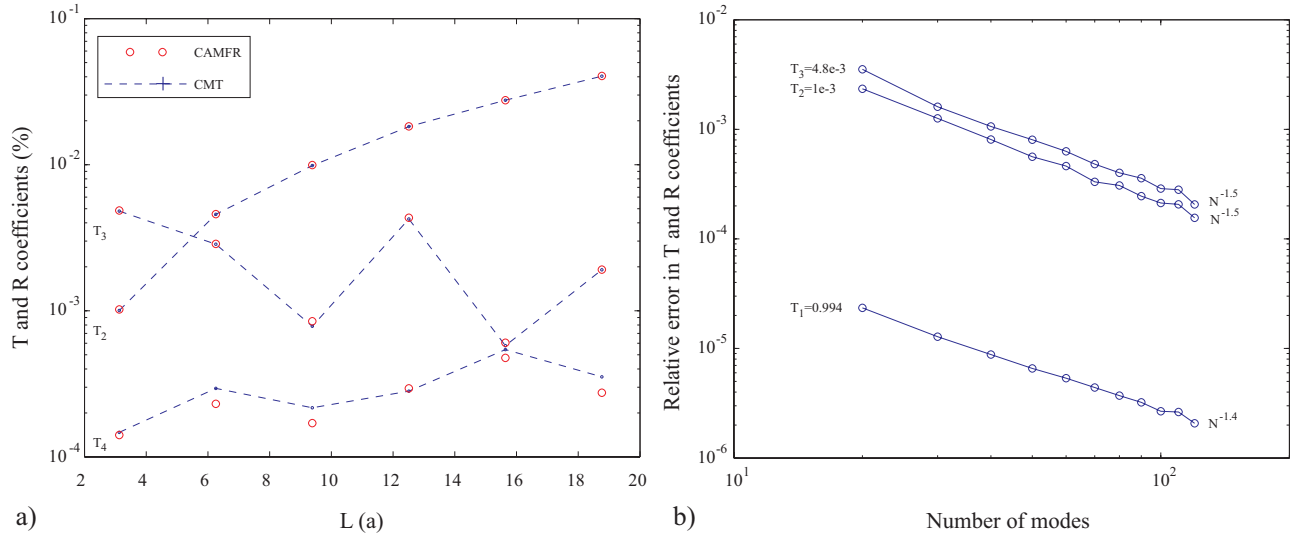
Figure 3. a) Transmitted powers T_2, T_3, T_4 in the second third and forth $m = 1$ modes for the grating lengths $[\frac{\Lambda}{2}, 3\Lambda]$ in the $\frac{\Lambda}{2}$ increments are plotted in crosses, calculated by our coupled mode theory. In this geometry the incoming and outgoing waveguides are the same. Results of an asymptotically exact transfer matrix based CAMFR code are presented in circles. When grating length is increased the power transfer to the phase matched first excited mode is monotonically increased as expected. b) Convergence of the errors in the transmitted and reflected coefficients for a grating of $L = \frac{\Lambda}{2}$ as a function of the number of expansion modes. Solid lines correspond to the relative errors in the transmission coefficients. Errors in the transmission and reflection coefficients exhibit faster than a linear convergence.

coefficients to a percent error with less then 40 basis functions.

Next, we consider a strong index-contrast sinusoidal Bragg grating variation of a waveguide profile where all the interfaces (including an outside metal jacket) are scaled by the same amount along the direction of propagation (see Fig. 1c)). A corresponding coordinate mapping will be that of (2) with $f(s) = \delta Sin(2\pi\frac{s}{\Lambda})$, where Λ is a period of the grating, and δ is its strength. We assume an infinite basic waveguide at $s < 0$ and $s > L$. Coupling elements are calculated from (5) with a selection rule $\Delta m = 0$. For a Bragg grating strength of $\delta = 0.05$ and a boundary condition of all the incoming radiation coming in the fundamental $m = 1$ mode we solve (4) for the power in the transmitted and reflected modes propagating in the incoming and outgoing waveguides. We choose the Bragg grating period Λ to match the beat length between the fundamental (transmission coefficient T_1) and a first excited mode (transmission coefficient T_2), so in the limit of long gratings all the power will be transferred to the excited mode. Expansion basis is the same as in previous study. On Fig. 3a) we plot in crosses the transmitted powers T_2, T_3, T_4 in the second, third and forth $m = 1$ modes for the grating lengths $[\frac{\Lambda}{2}, 3\Lambda]$ in the $\frac{\Lambda}{2}$ increments, as calculated by our CMT. For comparison, results of an asymptotically exact transfer matrix based CAMFR code[19] are presented on the same figure in circles exhibiting an excellent agreement with our results. When grating length is increased the power transfer to the first excited mode is monotonically increased as expected. On Fig. 3b), we present convergence of the transmitted and reflected coefficients for a sinusoidal taper of length $L = \frac{\Lambda}{2}$. Solid lines correspond to the relative errors in the transmission coefficients. Note a greater than linear convergence of our CMT with respect to the number of modes in the expansion basis. We also observe that our formulation gives the correct values of the main transmission and reflection coefficients to a percent error with less then 20 basis functions.

6. GVD AND DETERMINISTIC PMD OF MODES IN A HOLLOW OMNIDIRECTIONAL BRAGG FIBER.

Omnidirectional photonic bandgap fiber (OPBF) is a new class of Bragg fiber based on omnidirectional reflectivity.[1] The large hollow core of these fibers and the large index contrast in the surrounding omnidirectional mirror make the fiber to support a number of low-loss core-guided modes. Through deliberate fiber design
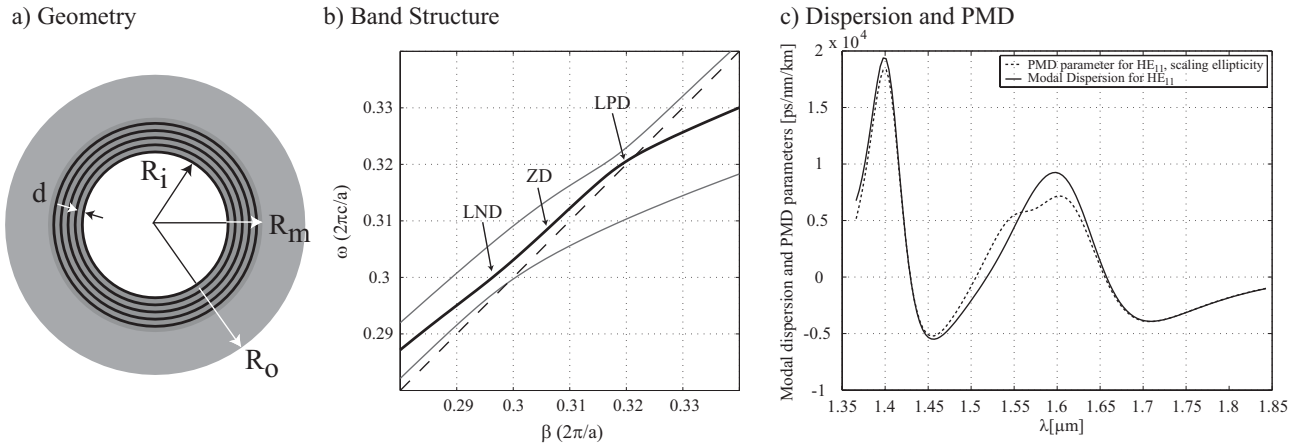
a) Geometry b) Band Structure c) Dispersion and PMD

Figure 4. (a) Schematic of omnidirectional photonic Bragg fiber. Hollow core of radius R_i, mirror region of N bilayers of thickness d, surrounded by an over-cladding extending to R_o. (b) Typical band structure of an OPBF. The diagonal dashed line is the air light line. To the left of the light line are guided modes of the core, while to the right are surface states of the mirror. The thick curve is the HE_{11} mode, exhibiting regions of large negative dispersion (LND), zero dispersion (ZD), and large positive dispersion (LPD). Thin lines are the nearby modes. (c) HE_{11} group-velocity dispersion D and PMD parameter for a uniform ellipticity perturbation. PMD tends to positively correlate with dispersion, especially in the high dispersion regions. However, low value of PMD, and considerable value of group-velocity dispersion can be simultaneously achieved by fiber design. At $\lambda = 1.51\mu m$, for example, PMD is zero while $D = -2000\frac{ps}{nm\ km}$.

one can tailor the fiber modes to exchange properties with other fiber modes over narrow frequency ranges (avoiding crossing), which gives these fibers rich, controllable dispersion properties. The dispersion properties of the OPBF fiber can be tailored very accurately, because of the large number of degrees of freedom the fiber geometry offers. This makes OPBF fibers good candidates for long-haul transmission, dispersion compensation, zero-dispersion transmission, or other applications that require accurate dispersion control. Intimately connected to the mode dispersion properties is the detrimental effects of Polarization Mode Dispersion (PMD). When dealing with potential applications like long-haul transmission or dispersion compensation, one must ensure that the PMD of a fiber is acceptably small. The aim of this section is to demonstrate dispersion and PMD properties of the modes of OPBFs.

OPBF consists of a hollow core, a series of bilayers of contrasting refractive-index glasses, and an over-cladding. Fig. 4a) illustrates the cross section of an OPBF. Modal electromagnetic fields decay exponentially in the mirror. Thus, field penetration into the mirror is largely limited to the first few bilayers. Moreover, the modal dispersion relation is very sensitive to the first several mirror layers. In fact, this sensitivity allows group-velocity dispersion control by design of such layers. For a particular realization of OPBF, the band structure of a doubly degenerate HE_{11} mode is shown in Fig. 4b. Data is presented in dimensionless units where a sets the length scale, ω is frequency, and β is propagation constant. Because of the avoided crossing with other guided modes, the HE_{11} dispersion curve exhibits regions of large negative dispersion, zero dispersion, and large positive dispersion.

Quantitative analysis of a mode's dispersion properties involves calculating a modal dispersion relation $\omega(\beta)$. For cylindrically symmetric dielectric fiber profiles, this can be accomplished by a well established transfer matrix technique.[1] Evaluation of the deterministic PMD (arising from uniform along the direction of propagation perturbations) is a much harder problem as it involves the change in the dispersion relation of an originally doubly degenerate mode when the waveguide geometry is perturbed away from cylindrical symmetry. In the case of low index-contrast waveguides, the problem of deterministic PMD evaluation was successfully solved in the context of coupled-mode theory in.[7] However, this formulation was found to fail in the case of high index-contrast. In the following, we apply CMT formulation derived in this paper to characterizing PMD of a doubly degenerate mode of an OBPF for a common elliptical perturbation of a high index-contrast fiber profile. We establish that, if in some range of frequencies a doubly degenerate mode of angular index $m = 1$

behaves like a mode of pure polarization TE or TM (where polarization is judged by the relative amounts of the electric and magnetic longitudinal energies in a modal crossection), its inter-mode dispersion parameter (which defines a deterministic PMD) $\tau = \frac{\partial \triangle \beta_e}{\partial \omega}$ is strongly correlated to the group-velocity dispersion D by $\tau = -\lambda \delta D$, where δ is a measure of the fiber ellipticity and $\triangle \beta_e$ is a split in the propagation constant of a linearly polarized doubly degenerate mode due to an elliptical perturbation. This indicates that regions of high dispersion will, generally, correlate with regions of high PMD. Thus, fiber design needs to be optimized to reduce PMD value when high group-velocity dispersion is desired.

In the case of a uniform circularly symmetric waveguide profile, eigen modes can be classified by their angular momentum number m and a propagation constant β. In cylindrical coordinate system $q^1 = \rho, q^2 = \theta$, $g^{0\rho\rho} = 1; g^{0\theta\theta} = \frac{1}{\rho^2}; g^{0zz} = 1; g^0 = \rho^2$, $\mathbf{F_0}(\rho, \theta, s) = \mathbf{F_0}(\rho)_\beta^m \exp(i\beta s + im\theta)$. We consider a general scaling perturbation that is uniform along $\hat{\mathbf{z}}$ axis (Fig. 1d)). Because of the uniformity of dielectric profile new fields can be characterized by a modified propagation constant $\tilde{\beta}$ and fields of the form $\mathbf{F}(\rho, \theta, s) = \mathbf{F}(\rho, \theta)_\beta \exp(i\beta s)$. When perturbed, discontinuous dielectric interfaces of radii ρ_i are described, by a new set of curves (2) $x = \rho_i Cos(\theta)(1+\delta_x), y = \rho_i Sin(\theta)(1+\delta_y)$, where $\theta \in (0, 2\pi), i \in (1, Number\ of\ interfaces)$. The case of $\delta_x = \delta_y = \delta$ corresponds to a uniform scaling, while the case of $\delta_x = -\delta_y = \delta$ corresponds to a uniform ellipticity of a waveguide profile. New eigen values $\beta^\pm$ of the split doubly degenerate eigen mode can be easily found by solving standard secular equations using coupling elements of (5):

$$\beta^\pm = \beta + \frac{< \psi_{\beta,m} | \triangle \hat{M} | \psi_{\beta,m} >}{< \psi_{\beta,m} | \hat{B} | \psi_{\beta,m} >} \pm \frac{< \psi_{\beta,m} | \triangle \hat{M} | \psi_{\beta,-m} >}{< \psi_{\beta,m} | \hat{B} | \psi_{\beta,m} >}. \tag{7}$$

PMD is defined to be proportional to the inter-mode dispersion parameter, which in terms of the group velocities mismatch is $\tau = \frac{1}{v_g^+} - \frac{1}{v_g^-}$. This can also be expressed as $\tau = \frac{\partial(\beta^+ - \beta^-)}{\partial \omega} = \frac{\partial(\triangle \beta_e)}{\partial \omega}$. Thus, in the case of a uniform scaling perturbation $\delta_x = \delta_y = \delta$, (5) gives $\triangle \beta_s = < \psi_{\beta,m} | \triangle \hat{M} | \psi_{\beta,m} > = 4\pi\delta\omega \int_{cros} d\rho d\theta(\epsilon|E_z|^2 + |H_z|^2)$, where integration is performed over the fiber cross section. Moreover, as shown in,[18] $\triangle \beta_s$ defines group-velocity dispersion through the following equalities $\triangle \beta_s = \delta(\omega \frac{\partial \beta}{\partial \omega} - \beta)$, $\frac{\partial \triangle \beta_s}{\partial \omega} = \delta\omega \frac{\partial^2 \beta}{\partial \omega^2} = -\lambda \delta D$.

Next, consider the case of a uniform ellipticity perturbation $\delta_x = -\delta_y = \delta$. The first-order correction to the split in the values of propagation constants of the modes $(\beta, m = 1)$ and $(\beta, m = -1)$ due to the uniform ellipticity is $\triangle \beta_e = 2 < \psi_{\beta,1} | \triangle \hat{M} | \psi_{\beta,-1} > = 4\pi\delta\omega \int_{cross} d\rho d\theta[(-\epsilon|E_z|^2 + |H_z|^2) + 2Im(\epsilon E_r^* E_\theta - H_r^* H_\theta)]$, where E's and H's are the electromagnetic fields of the $(\beta, m = 1)$ mode. In general, we find that for high index-contrast waveguides $\triangle \beta_e$ is dominated by the diagonal term $\sim \int_{cros} d\rho d\theta[(-\epsilon|E_z|^2 + |H_z|^2)]$, while for low index contrast waveguides the cross terms become equally important.

An important conclusion about PMD of a fiber can be drawn when electric or magnetic longitudinal energy dominates substantially over the other.[18] In the case of pure-like TE ($\int_{cros} d\rho d\theta \epsilon |E_z|^2 \ll \int_{cros} d\rho d\theta |H_z|^2$) or TM ($\int_{cros} d\rho d\theta |H_z|^2 \ll \int_{cros} d\rho d\theta \epsilon |E_z|^2$), the mode split due to the uniform scaling becomes almost identical to the split in the degeneracy of the modes due to the uniform ellipticity perturbation. Thus $\triangle \beta_s \simeq \triangle \beta_e$. As PMD is proportional to $\tau = \frac{\partial \triangle \beta_e}{\partial \omega}$, and taking into account expressions for the frequency derivatives of $\triangle \beta_s$ we arrive at the conclusion that for such modes PMD is proportional to the group-velocity dispersion of a mode

$$\tau = \frac{\partial \triangle \beta_e}{\partial \omega} \simeq \frac{\partial \triangle \beta_s}{\partial \omega} = -\lambda \delta D. \tag{8}$$

In Fig. 4c), we present the HE_{11} group-velocity dispersion D and a PMD parameter defined as $-\frac{\tau}{\lambda \delta}$ for a uniform ellipticity perturbation and a particular design of an OBPF. As predicted by (8), the PMD of the mode follows the group-velocity dispersion closely, especially in the high-dispersion regions around $1.4\mu m, 1.45\mu m, 1.6\mu m, 1.7\mu m$. In the moderate-dispersion region around $1.51\mu m$, PMD and dispersion can be decoupled so that a low value of PMD and a still considerable value of the modal geometric dispersion $-2000 \frac{ps}{nm\ km}$ are achieved.

7. TAPERS IN 2D PHOTONIC CRYSTAL WAVEGUIDES

We conclude with a coupled mode theory analysis of radiation scattering in a 2D photonic crystal taper. On Fig. 5a) schematic of a taper between a $r_g = 0.2a$ line defect waveguide in a square lattice of $r_x = 0.3a$ dielectric
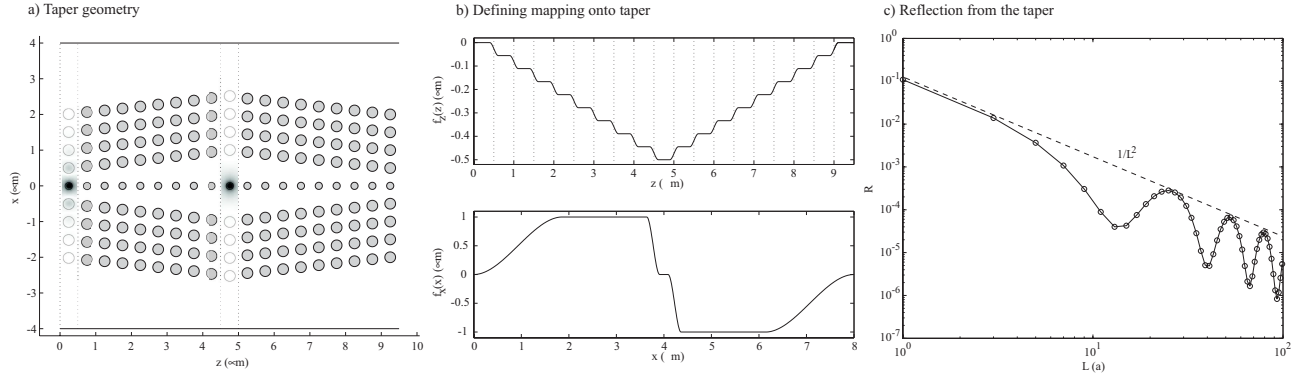
Figure 5. (a) Schematic of a taper between a $r_g = 0.2a$ line defect waveguide in a square lattice of $r_x = 0.3a$ dielectric rods in air and a 1D sequence of dielectric rods $r_g = 0.2a$. It is assumed that to the left and to the right of the taper the photonic crystal waveguide is unperturbed and described by the first unit cell of the schematic. Distribution of the electric field energy is presented in the first unit cell and in the middle of the taper for $\omega = 0.25 \times 2\pi c/a$. (b) Functions defining the mapping of the dielectric interfaces of an unperturbed photonic crystal waveguide onto a taper. (c) Reflected power form the taper at $\omega = 0.25 \times 2\pi c/a$ as a function of taper length L. Observe a $1/L^2$ decrease of the reflected power with taper length.

rods in air and a 1D sequence of dielectric rods $r_g = 0.2a$ is presented, where a defines periodicity of the photonic crystal waveguide in the direction of propagation. All the dielectric rods have index $n = 3.37$. To the left and to the right of the taper the photonic crystal waveguide is unperturbed and described by the first unit cell of the schematic. Transmission through such a taper for TE polarization (electric field is out of plane) has been studied previously in the instantaneous mode framework[13] where coupled mode theory was constructed using a large number instantaneous modes calculated at closely spaced intervals along the propagation direction. The frequency $\omega = 0.25 \times 2\pi c/a$ is chosen so that the waveguide formed by the sequence of dielectric rods is singlemoded, while a photonic crystal waveguide is also singlemoded guiding in the band gap regime. We again used CAMFR code to compute an expansion basis constructed of the eigen modes of an unperturbed photonic crystal waveguide defined by the first cell on the Fig. 5a). Total 4 propagating modes with real propagation constants and 40 evanescent modes with complex propagation constants were used in the basis. We found, however, that only the 2 counter-propagating guided modes of the unperturbed photonic crystal waveguide contributed mostly to the scattering. We then defined an analytic mapping of the dielectric profile of an unperturbed photonic crystal waveguide onto a tapered photonic crystal using the following mapping $\tilde{x} = x + f_x(x)f_z(z), \tilde{z} = z$, where $f_x(x)$ and $f_z(z)$ were chosen to be as on Fig. 5b), and where (x, z) are defined an unperturbed waveguide profile. Finally, on Fig. 5c) we plot reflected power form the taper at $\omega = 0.25 \times 2\pi c/a$ as a function of taper length L, and observe an expected $1/L^2$ decrease of the reflected power with taper length. Advantage of our coupled mode theory is the use of a single expansion basis at all points along the propagation direction which can be of great advantage for computationally demanding 3D simulations.

8. CONCLUSION

In this work, we presented a novel form of the coupled mode and perturbation theories to treat geometric variations of generic waveguide profiles with an arbitrary dielectric index contrast. This formulation, unlike much previous work, holds equally well for high index contrast. We demonstrated that for general scaling variations (including tapers and Bragg gratings) of high index-contrast profiles our method exhibits a faster than linear convergence with the number of expansion modes. Applications to various aspects of light propagation in deformed photonic crystal fibers and 2D waveguides were demonstrated.

REFERENCES

1. Steven G. Johnson, Mihai Ibanescu, M. Skorobogatiy, Ori Weisberg, Torkel D. Engeness, Marin Soljačić, Steven A. Jacobs, J. D. Joannopoulos, and Yoel Fink, "Low-loss asymptot-

ically single-mode propagation in large-core OmniGuide fibers," Opt. Express **9**, 748 (2001), http://www.opticsexpress.org/abstract.cfm?URI=OPEX-9-13-748.

2. Steven G. Johnson, Mihai Ibanescu, M. Skorobogatiy, Ori Weisberg, J. D. Joannopoulos, and Yoel Fink, "Perturbation theory for Maxwell's equations with shifting material boundaries," Phys. Rev. E **65**, 66611 (2002).

3. M. Skorobogatiy, Mihai Ibanescu, Steven G. Johnson, Ori Weisberg, Torkel D. Engeness, Marin Soljačić, Steven A. Jacobs, and Yoel Fink, "Analysis of general geometric scaling perturbations in a transmitting waveguide: fundamental connection between polarization-mode dispersion and group-velocity dispersion," J. Opt. Soc. Am. B **19**, (2002).

4. M. Skorobogatiy, Steven A. Jacobs, Steven G. Johnson, and Yoel Fink, "Dielectric profile variations in high index-contrast waveguides, coupled mode theory and perturbation expansions," Phys. Rev. E **67** ,46613 (2003).

5. M. Lohmeyer, N. Bahlmann, and P. Hertel, "Geometry tolerance estimation for rectangular dielectric waveguide devices by means of perturbation theory," Opt. Communications **163**, pp. 86–94 (1999).

6. N. R. Hill,"Integral-equation perturbative approach to optical scattering from rough surfaces," Phys. Rev. B **24**, p. 7112 (1981).

7. D. Marcuse, *Theory of dielectric optical waveguides* (Academic Press, 2nd ed., 1991).

8. A. W. Snyder and J. D. Love, *Optical waveguide theory* (Chapman and Hall, London, 1983).

9. B. Z. Katsenelenbaum, L. Mercader del Río, M. Pereyaslavets, M. Sorolla Ayza, and M. Thumm, *Theory of Nonuniform Waveguides: The Cross-Section Method* (Inst. of Electrical Engineers, London, 1998).

10. L. Lewin, D. C. Chang, and E. F. Kuester, *Electromagnetic waves and curved structures* (IEE Press, Peter Peregrinus Ltd., Stevenage 1977).

11. F. Sporleder and H. G. Unger, *Waveguide tapers transitions and couplers* (IEE Press, Peter Peregrinus Ltd., Stevenage 1979).

12. H. Hung-Chia, *Coupled mode theory as applied to microwave and optical transmission* (VNU Science Press, Utrecht 1984).

13. Steven G. Johnson, P. Bienstman, M. A. Skorobogatiy, M. Ibanescu, E. Lidorikis, and J. D. Joannopoulos "The adiabatic theorem and a continuous coupled-mode theory for efficient taper transitions in photonic crystals," Phys. Rev. E **66**,66608 (2002).

14. R. Holland, "Finite-difference solution of Maxell's equation in generalized nonorhogonal coordinates," IEEE Trans. Nucl. Sci. **30**, 4589 (1983).

15. J.P. Plumey, G. Granet, and J. Chandezon, "Differential covariant formalism for solving Maxwell's equations in curvilinear coordinates: oblique scattering from lossy periodic surfaces," IEEE Trans. on Antennas Propag. **43**, 835 (1995).

16. E.J. Post, *Formal Structure of Electromagnetics* (Amsterdam: North-Holland, 1962).

17. F.L. Teixeira and W.C. Chew, "Analytical derivation of a conformal perfectly matched absorber for electromagnetic waves," Microwave Opt. Technol. Lett. **17**, 231 (1998).

18. M. Skorobogatiy, Steven A. Jacobs, Steven G. Johnson, and Yoel Fink, "Geometric variations in high index-contrast waveguides, coupled mode theory in curvilinear coordinates," Opt. Express **10**, 1227 (2002), http://www.opticsexpress.org/abstract.cfm?URI=OPEX-10-21-1227.

19. P. Bienstman, software at http://camfr.sf.net.